

PROTON ACCELERATION TEST WITH A SCRFQ

S. Arai, T. Fukushima, T. Morimoto, E. Tojyo, N. Tokuda and M. Yoshizawa
Institute for Nuclear Study, University of Tokyo, Tanashi-shi, Tokyo 188

T. Hattori

Tokyo Institute of Technology, Ohokayama, Meguro-ku, Tokyo 152

Abstract

A proton accelerating model working at frequency of 50 MHz has been constructed to evaluate the overall performance of a split coaxial RFQ with modulated vanes. Through the beam test, it is confirmed that the accelerating performance of the RFQ almost agrees with the expected one.

1. Introduction

A split coaxial RFQ (SCRFQ) has been developed at Institute for Nuclear Study for acceleration of the very heavy ions with the charge-to-mass ratio larger than 1/60. In order to make it easy to install four vanes in the RFQ, a multi-module cavity structure was employed [1]. As the first step of the development, a cold model with flat vanes, excited in a frequency range of 37 ~ 41 MHz, was fabricated to investigate experimentally the mechanical and rf characteristics [2]. Through the experiments, it was verified that the precise vane alignment, good mechanical stability and the required field distribution were achieved. Furthermore, an equivalent circuit analysis was developed to explain theoretically the longitudinal field distribution in the fundamental and higher-harmonics modes and the dispersion characteristics of the resonator [3].

As the second step, a proton accelerating model working at a frequency of 50 MHz was constructed to evaluate the overall performance of the multi-module split coaxial RFQ. In the beam tests with the low-current beam, we measured the output energy, the energy spread, the transmission efficiency and the output-beam emittance.

2. Proton Accelerating Model

The cold model was converted into a proton accelerating model by replacing the flat vanes with modulated vanes. The accelerating model, about 2 m in total length and 0.4 m in diameter, consists of four-module cavities. The modulated vanes of about 2 m in length were completed by connecting the short-vane pieces of 20 cm long. The material of the vanes is aluminum alloy, while the cavity cylinders were made of brass. The measured unloaded Q-value is 2230, and this value corresponds to a resonant resistance of 18.3 k Ω . The vanes were aligned with accuracy better than ± 0.1 mm; the azimuthal field unbalance between quadrants was less than $\pm 1\%$.

Main vane parameters are summarized in table 1. The vanes were designed by laying emphasis on high acceleration rate rather than high beam current. Total number of cells, including radial matching section of 10 cells, is 168. The injection energy was set at a relatively low value of 2 keV.

3. Beam Acceleration Test

The beam acceleration test was performed under the pulse operation with a repetition of 400 pps. The pulse width of the rf is 200 μ s and that of the beam is 100 μ s. The layout of the test stand is shown in fig. 1. Protons, a few μ A in peak current, were produced by a compact ion source of ECR type. The beam, which passed through an ion separating magnet, was matched to the RFQ acceptance by means of an einzel-lens doublet, an electric-quadrupole triplet, and an einzel-lens singlet. The beam current was measured with Faraday cups.

Transmission was measured as a function of the rf voltage by injecting the beam with an emittance as shown in fig. 2. The result is shown in fig. 3. Solid points express the ratio of the accelerated-beam current to the input-beam current. Accelerated-beam current was measured with the Faraday cup located downstream of the analyzer magnet. The open circles express the transmission of the beam including the unaccelerated particles. This was measured with the Faraday cup at the exit of the RFQ. The transmission of accelerated beam is about 84% at a design voltage and agrees with a calculated one.

The output-beam emittances were measured by means of an emittance monitor, in which two slits were set at a space of 446 mm. The result is shown in fig. 4. By comparing figs. 2 and 4, it became clear that the output emittance is approximately equal to a calculated one, even though the input emittance is smaller than the calculated one.

Output beam energy was measured by means of a magnetic spectrometer with a bending angle of 90 degrees. The energy resolution of the spectrometer was $\pm 0.4\%$, when a slit width was set for ± 1 mm. Spectra of output beam energy were measured for four values of rf voltage. The obtained energy spectra are shown in fig. 5. In this region of the rf voltage, the shape of the spectrum changed hardly, but the energy spread increased as the rf voltage increased. The energy at the peak point of spectrum was 60 keV and the energy spread at a rf voltage of 3.05 kV was about $\pm 1.8\%$ in full width at half maximum. They almost agree with the designed values: 59.6 keV and $\pm 2.4\%$ in full width.

5. Concluding Remarks

As for the field distribution in the SCRFBQ, there is no problem. Through the beam test, it was confirmed that the accelerated beam energy, energy spread, transmission efficiency and output beam emittance agreed approximately with the designed values.

References

- [1] S. Arai, GSI-Report 83-11 (1983).
- [2] E. Tojyo *et al.*, Proc. 1986 Linear Acc. Conf., SLAC-303 (1986) 374.
- [3] S. Arai, INS-T-464 (Accelerator-4) (1986).

Table 1 Vane Parameters of a Proton Accelerating Model

Frequency (f)	50	MHz
Kinetic energy (T)	2.00 - 59.6	keV
Normalized emittance (ϵ_N)	0.03	π cm·mrad
Intervane voltage (V)	2.9	kV
Focusing strength (B)	3.8	
Max. defocusing strength (Δ_b)	-0.075	
Synchronous phase (ϕ_s)	-90 - -30	deg
Max. modulation (m_{max})	2.48	
Number of cells (radial matcher)	168 (10)	
Vane length	205.19	cm
Mean bore radius (r_0)	0.541	cm
Min. bore radius (a_{min})	0.294	cm
Margin of bore radius (a_{min}/a_{beam})	1.15	
Transmission (0 emA)	84	%
(2 emA)	69	%
(4 emA)	56	%

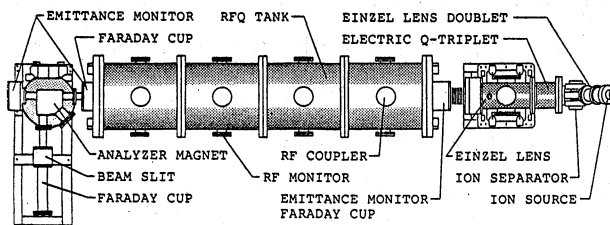


Fig. 1 Layout of a beam test stand.

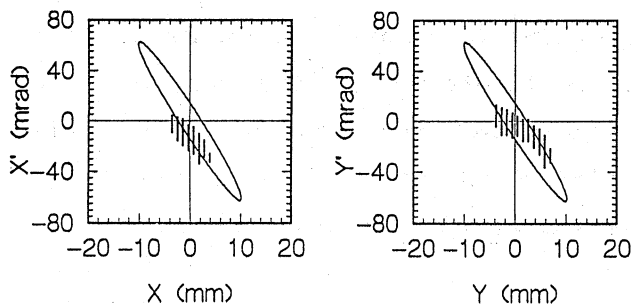


Fig. 2 Phase-space projections of the input beam. Bars show the experiments (90% contour) and ellipses show the calculations.

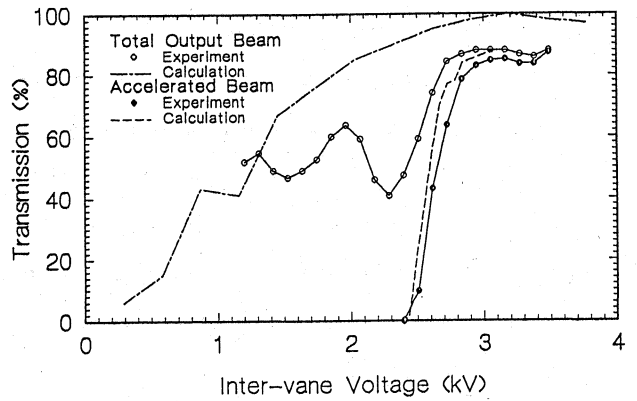


Fig. 3 Transmissions measured as a function of the rf voltage.

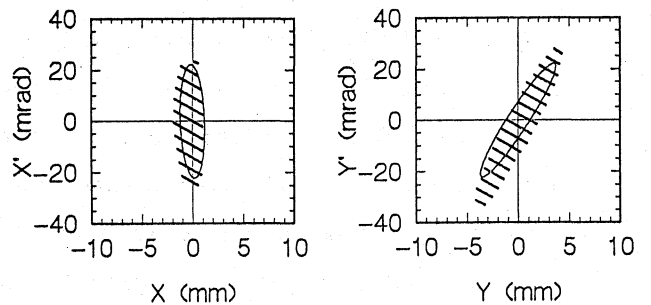


Fig. 4 Phase-space projections of the output beam.

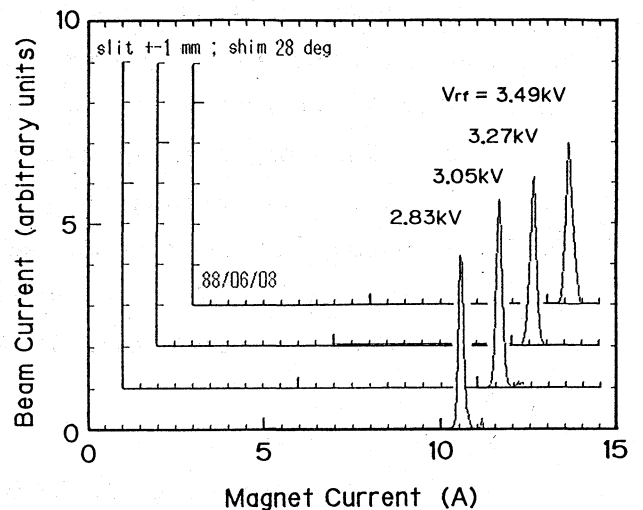


Fig. 5 Energy spectra of the output beam.